Collective coupling between pairing and rotational degrees of freedom within a simple model

P. Quentin [1,2,3,*] and J. Bartel[4]

[1]*Division of Nuclear Physics, Advanced Institute of Materials Science, Ton Duc Thang University, Ho Chi Minh City, Vietnam*

[2]*Faculty of Applied Sciences, Ton Duc Thang University, Ho Chi Minh City, Vietnam*

[3]*CENBG, UMR5797, Université de Bordeaux, CNRS-IN2P3, Gradignan, France*

[4]*IPHC, UMR7178, Université de Strasbourg, CNRS-IN2P3, Strasbourg, France*

(Received 28 December 2019; revised 6 July 2020; accepted 9 September 2020; published 4 November 2020)

A simple model to study the collective coupling between pairing and rotational degrees of freedom in well-deformed even-even nuclei is proposed. It relies on the description of the effects of pairing correlations on the rotational motion in terms of intrinsic vortical currents. As a result, an expression of the rotational energy within a band is provided as a polynomial of order three in the square of the angular velocity. The coefficients of this polynomial have a well-defined analytical form and their values are determined from merely three experimental pieces of data: the energy of the first 2^+ state, the ground-state charge quadrupole moment as deduced from $B(E2, 2^+ \rightarrow 0^+)$ measurements, and a quantity deduced from the odd-even mass differences in neighboring odd nuclei. This model is tested in 24 deformed nuclei chosen across the rare-earth and actinide regions. In spite of the very restricted input of data, and moreover which is limited to nuclear properties at zero or very low excitation energies, the agreement with the data within the yrast line is in many cases, especially in actinide nuclei, excellent up to angular momenta of the order of $30\hbar$ or more. Of course, such an approach is by construction unable to reproduce physical effects which do not result from this Coriolis antipairing (CAP) type of collective quenching of pairing correlations. This is especially the case in the rare-earth region, where a backbending effect is often observed. In such cases our model may be considered as a baseline in order to disentangle the effect of the CAP collective mode from those of other existing spectroscopic phenomena.

DOI: 10.1103/PhysRevC.102.054305

I. INTRODUCTION

The concept of rotational bands has been introduced in physics through the infrared-absorption studies of diatomic molecules [1]. Such an energy spectrum exhibits, as is well known, an $I(I+1)$ variation corresponding to states having angular momenta $\hbar I$ in so far as the three angular variables defining the inertia frame are solely involved. In actuality, couplings to various other degrees of freedom perturb this ideal spectral scheme. These couplings belong to two categories: some are of a collective nature (such as gradual weakening of pair correlations, centrifugal stretching, and coupling to collective vibrations), others more related to single-particle degrees of freedom (such as rotation-induced changes in the mean field and sudden occurrences of single pair breaking).

To describe these spectra, setting apart numerous microscopic calculations of various kinds (shell-model calculations, Routhian Hatrtree-Fock-Bogoliubov and corresponding relativistic approaches) one has developed purely phenomenological approaches dubbed at the beginning [2] "variable moment of inertia" (VMI) approaches. One possible formal frame under those lines is to embed such a variation in a truncated expansion of the rotational energies in powers of $I(I+1)$. Casten [3] has shown that the inclusion of the second-order term could be connected in some cases with a coupling between the ground and gamma bands in reasonably well deformed nuclei. In a complementary approach initiated by Harris [4] one considers an expansion $E(\Omega)$ of the rotational energy as a power series of the angular velocity Ω and perform a fit of its parameters.

In the present study we aim at providing a polynomial expression for $E(\Omega)$ in well-deformed even-even nuclei, à la Harris thus, but whose algebraic form is deduced from an underlying dynamical property and which includes only a limited amount of experimental information, namely, the energy of the first 2^+ state, together with the ground-state quadrupole deformation and some measure of the amount of ground-state pairing correlations. It relies on consideration of the coupling between pairing correlations for all Cooper pairs with the global rotation (at least up to moderate spin values) leading to a substantial reduction of the moments of inertia from their rigid-body values. This effect was deemed in the seminal paper of Bohr, Mottelson, and Pines [5] as one clear indicator of the existence of pairing correlations in low-lying nuclear states, which was later confirmed theoretically by Migdal [6] within the framework of time-dependent Green's functions and by Belyaev [7] and Nilsson and Prior [8] within a non-self-consistent version of the adiabatic time-dependent Hartree-Fock-Bogolyubov approximation. It results from the Pauli principle quenching of pairing correlations due to the existence of particle-hole excitations generating the rotational collective mode. Explicit early calculations both purely

*philippe.quentin@tdtu.edu.vn

phenomenological [9] or using the Belayev formula [10] substantiated these theoretical findings.

Of particular interest for our study was the recognition by Mottelson and Valatin [11] of this effect as an explicit intrinsic collective mode known as the Coriolis antipairing (CAP) mode. It corresponds to a gradual collective reduction of the pair correlations similar (upon making the standard connection between the Lorentz force and the Coriolis pseudoforce) to the response of a type-I superconductor immersed in a magnetic field.

Recent successful phenomenological descriptions of rotational bands in well-deformed heavy nuclei have been produced by using a rather simple yet effective parametrization of the CAP effect [12,13]. This approach has been pursued upon including, in an equally simple way, the possibility of some centrifugal stretching [14]. This rotation-induced possible deformation has been tested in well-deformed nuclei of the actinide region. As a result, it does not seem to play there a crucial role for the nuclear states studied.

In our present study, the rotational pair-correlation quenching is interpreted as resulting from the generation, in a pair-correlated fluid, of intrinsic vortical currents which are counter rotating with respect to the global rotation observed in the laboratory frame. This work is rooted in the theoretical approach developed in Ref. [15], where it is shown that the counter-rotating intrinsic currents which are generated by pairing correlations can be very well described by an intrinsic vortical mode proposed within the so-called Chandrasekhar's S-ellipsoid dynamics [16].

The paper is organized as follows: The model in use for the rotational energy is presented in Sec. II and the determination of its parameters is the subject of Sec. III. In Sec. IV, the relation within our theoretical framework between the angular velocity and the angular momentum is established. Finally, the results of our model for the variation, within a band, of the excitation energies and the kinematic moments of inertia with respect to the angular momentum or angular velocity are presented and discussed for an extended sample of well-deformed even-even nuclei in Sec. V, with some conclusions drawn in Sec. VI.

Note that some preliminary accounts of the present approach have been briefly discussed in Refs. [14,17].

II. THE MODEL

A. The velocity field

Within the S-ellipsoid description of fluid dynamics, one introduces a divergence-free, and thus nondeforming, linear intrinsic velocity field. It induces a dynamical mode which may be described as resulting from the product of three geometrical transformations (as explained in Ref. [18]) for a fluid contained in a spheroid having Oz as symmetry axis:

(a) a volume-conserving scaling $\hat{S}$ of the spheroidal volume of the fluid container (supposed here to be axially symmetric) into a spherical shape;
(b) a uniform rotation $\hat{R}$ of the fluid with a rotation axis perpendicular to the Oz axis, e.g., the Ox axis, with angular velocity ω;
(c) a scaling of both the coordinate and the velocity vectors, which is just the inverse of $\hat{S}$ from the previous spherical shape back into the initial spheroid.

This intrinsic collective mode is then coupled to a global rotation around the same axis perpendicular to the Oz axis, e.g., the Ox axis, with angular velocity Ω with respect to the laboratory frame. The nature of this coupling when applied to the rotation of a pairing-correlated nuclear state is investigated within a model where the angular velocity ω of the vortical mode appears as a function of the angular velocity Ω of the global rotation.

The dependence of ω on Ω (see, e.g., Ref. [15]) should first be such that the product $\omega\Omega$ is negative corresponding to the counter-rotational character of this intrinsic mode.

All other things being kept constant, the absolute value of the angular velocity ω should be an increasing function of Ω since the pair correlation counter-effect should be an increasing function (taken here as linear) of its cause, namely, the global rotation.

All other things being kept constant, the absolute value of the angular velocity ω should also be an increasing function of the so-called pair condensation energy $E_{\rm cond}$, defined as the absolute value of the expectation value of the residual interaction in the considered nuclear state. This expectation value is sometimes, in the context of nuclear physics, merely referred to as the pairing energy, as in the seminal paper [19], which must not be confused with the correlation energy, which is the gain in energy due to the presence of correlations with respect to an uncorrelated solution.

This dependence of ω on $E_{\rm cond}$ is due, again, to the fact that the pair correlation counter-effect should be an increasing function (taken here as linear) of its cause, namely, a quantity related to the intensity of pair correlations. This quantity is a decreasing function of Ω which is assumed (as in the simple model of Ref. [15]) to have a quadratic behavior as

$$E_{\rm cond}(\Omega) = E_{\rm o}\left[1 - \left(\frac{\Omega}{\Omega_c}\right)^2\right] = E_{\rm o}[1-\xi^2], \quad \xi = \frac{\Omega}{\Omega_c}, \quad (1)$$

where $E_{\rm o}$ is the pair condensation energy at zero angular momentum and Ω_c is the critical angular velocity where pairing correlations vanish. The above dependence of $E_{\rm cond}$ on Ω can be justified as follows: Due to the already advocated mathematical similarity between the Lorentz force and the Coriolis pseudoforce, one can take stock of the behavior of the energy qap in the vicinity of the superfluid-normal first-order phase transition, as a function of the temperature, in superconductors (see, e.g., Ref. [20]), and postulate that its variation $\Delta(B)$ as a function of the norm B of the magnetic field is given from its zero-field value $\Delta(0)$ as:

$$\frac{\Delta(B)}{\Delta(0)} = \left[1 - \left(\frac{B}{B_c}\right)^2\right]^{1/2}, \quad (2)$$

where B_c is the critical field value for the transition from the superconducting phase to the normal phase. This, replacing the norm B of the magnetic field and its critical value B_c by Ω and Ω_c, leads to Eq. (1) upon noting that, in the seniority force model approximation, the energy $E_{\rm cond}$ is proportional to the square of Δ.

From the above, we thus propose

$$\omega = -k\Omega[1-\xi^2], \tag{3}$$

where k is a positive constant to be determined below.

It is our contention that the critical angular velocity Ω_c should depend on the level of correlations in the ground state, i.e., at zero angular momentum. Let us denote in what follows the pair condensation energy $E_{\rm cond}$ as a function of Ω by $E_{\rm cond}(\Omega)$ and by $\mathcal{J}_c$ the critical value (i.e., for $\Omega = \Omega_c$) of the moment of inertia. For such a critical angular velocity, the pairing correlations are vanishing, by definition, and thus $E_{\rm cond}(\Omega_c) = 0$. For finite systems as atomic nuclei, we do know that, of course, there is no such thing as a sharp cutoff of these correlations. This is a model approximation shared by most, if not all, of the current microscopic description of rotating nuclei. At any rate, our approach is not designed to describe such situations and the concept of criticality serves here only to model the behavior of the function $\omega(\Omega)$ at values of Ω significantly smaller than Ω_c in most cases.

It is appropriate to approximate the moment of inertia $\mathcal{J}_c$, thus in absence of pairing correlations, by its rigid-body value $\mathcal{J}_R$, known to be well represented by its semiclassical, or liquid drop model, value. The effect of the nuclear deformation should be taken into account, through some appropriate parametrization (using here the usual quadrupole parameter β or the semi-axis ratio q within an axially symmetrical description in terms of an ellipsoid).

The precise definition of Ω_c will result in the theory of superconductivity (for B_c in that case) from a relation between the critical rotational energy $E_c^{\rm rot} = 1/2\mathcal{J}_c\Omega_c^2$ and the pair condensation energy at zero angular velocity, $E_{\rm cond}(0) = E_{\rm o}$, as discussed in the forthcoming Sec. III A.

B. Collective energy

As in Ref. [15] we assume a quadratic expression for the total excitation energy as a function of the two angular velocities Ω and ω, corresponding thus to a low-velocity ansatz,

$$E(\omega,\Omega) = \tfrac{1}{2}[A\omega^2 + 2B\Omega\omega + C\Omega^2], \tag{4}$$

in terms of generalized moments of inertia A, B, and C to be defined below.

Using now Eq. (3) in Eq. (4), one obtains the total excitation energy $E(\Omega)$ as a function of Ω:

$$E(\Omega) = \frac{\Omega^2}{2}[C - 2Bk(1-\xi^2) + Ak^2(1-\xi^2)^2]. \tag{5}$$

According to Ref. [18] the generalized moments of inertia A, B, and C can be evaluated semiclassically (up to second-order terms in $\hbar$ similarly to what has been done in Ref. [21] for the global rotation) as

$$A = \eta\Theta\left[1 - \frac{D}{\eta}\Theta\right], \quad B = \eta\left[1 - \frac{D}{\eta}\Theta\right],$$
$$C = \eta\Theta\left[1 - \frac{D}{\eta\Theta}\right], \tag{6}$$

where

$$\eta = \mathcal{J}_R^{\rm o} q^{1/3}, \quad \Theta = \frac{1}{2}\left(q + \frac{1}{q}\right), \tag{7}$$

$$D = -m(3\pi^2)^{-2/3}\sum_{\nu=n,p}\iiint f_\nu(\vec{r}\,)\rho_\nu^{1/3}(\vec{r}\,)d^3r, \tag{8}$$

and where $\mathcal{J}_R^{\rm o}$ is the rigid-body moment of inertia for a spherical nuclear shape, and $q = c_z/c_\perp$ is the ratio of the semi-axis of the nuclear shape (approximated as being of a spheroidal type) along the symmetry z axis to that along the perpendicular direction. The function Θ is minimal at the sphericity where $\Theta(1) = 1$. The latter thus entails that $B \leqslant A \leqslant C$. Note, in passing, that the moment of inertia $\mathcal{J}_R$ corresponding to a rigid-body rotation is given by C.

The definition of the above constant D contains the isoscalar nucleon effective mass form factor in a finite nucleus $f_\nu(\vec{r}\,) = m/m_\nu^*(\vec{r}\,)$, and the corresponding density distribution $\rho_\nu(\vec{r}\,)$ (where $\nu = \{n, p\}$ stands for the nucleon charge state). It has been shown in Ref. [18] that the ratio D/η can quite accurately be approximated by

$$\frac{D}{\eta} = 5\left(\frac{8}{9\pi}\right)^{2/3} f_{\rm NM}\mathcal{A}^{-2/3}, \tag{9}$$

where $f_{\rm NM} = m/m_{\rm NM}^*$ is the (constant) isoscalar nucleon effective-mass form factor in nuclear matter and where $\mathcal{A}$ is the total number of nucleons. For a spherical nucleus one has $A = B = C = \eta(1 - \frac{D}{\eta})$. One gets, e.g., for $\mathcal{A} = 240$ $D/\eta = 0.07$, upon using the Skyrme SkM* interaction [22] where $f_{\rm NM} = 1.27$.

Now, an important remark is in order. In Ref. [21] one has evaluated the semiclassical corrections beyond the classical Thomas-Fermi moment of inertia (for the global rotation). These come, indeed, from two sources. One stems from a paramagnetic coupling of the rotation with the spin degrees of freedom; the other, of a diamagnetic nature, is related to the orbital motion in the nuclear surface. As it turns out, both effects correspond roughly to the same order of magnitude (in absolute values). Actually, the orbital contribution is generally weaker than its spin counterpart. In Ref. [21] it was found that the relevant moment of inertia at sphericity is given by

$$C = \mathcal{J}_R^{\rm o}[1 + (\zeta_l + \zeta_s)\mathcal{A}^{-2/3}], \tag{10}$$

where $\mathcal{J}_R^{\rm o}$ is the Thomas-Fermi (rigid-body) moment of inertia and where for the Skyrme SkM* interaction, one has obtained

$$\zeta_l \approx -1.9, \quad \zeta_s \approx 2.6, \tag{11}$$

for the orbital and spin correction terms, respectively. One may wonder how these figures depend on the particular effective interaction under consideration. First, the absolute value of the orbital diamagnetic corrective term D/η is inversely proportional to the effective mass in nuclear matter. We thus expect its contribution to be slightly larger, for instance, with the SIII parametrization [23] than with SkM* [22] (with $m^\star/m = 0.76$ for the former and 0.79 for the latter). On the other hand, the magnitude of the paramagnetic spin correction clearly depends on the spin susceptibility (see Table 2

of Ref. [21], where one observes significant variations of this quantity for a sample of commonly used Skyrme force parametrizations. For the sake of simplicity and in view of the small size of the corrections involved, we will, in what follows, merely use the SkM* interaction as a reference (well suited, as is well known, to describe large deformation properties) for the underlying microscopic calculations. We will thus consistently use for the values of the effective mass in nuclear matter, of the spherical rigid body moments of inertia (see below) and of the above-defined corrective terms (ζ_l, ζ_s) what is obtained when using this Skyrme force parametrization.

Notice that, in the semiclassical calculations yielding the above expressions for the generalized moments A, B, and C, one has ignored, as already mentioned, the spin degrees of freedom. As a consequence, the reduction of their value at sphericity by $1 - \frac{D}{\eta} \approx 7.6\%$ for, e.g., $\mathcal{A} = 240$ and the SkM* force, is spurious. We propose therefore to renormalize the above-given expressions so as to have at sphericity the moment of inertia C (and consequently A and B as well) corrected from their Thomas-Fermi values with the corrective terms of Eqs. (10), and (11). This is achieved by multiplying in what follows the generalized moments A, B, and C by a factor

$$F = \frac{1 + 0.69\mathcal{A}^{-2/3}}{1 - \frac{D}{\eta}} \tag{12}$$

in such a way that one gets, for instance, for the generalized moment A,

$$A = \eta\Theta F \left[1 - \frac{D}{\eta}\Theta\right], \tag{13}$$

and similar expressions for B and C according to Eqs. (6).

From the semiclassical ETF study of Ref. [21] we know that, when using the Skyrme SkM* effective interaction, a fairly good estimate of the rigid-body moment of inertia $\mathcal{J}_R^{\rm o}$ is given by

$$\frac{\mathcal{J}_R^{\rm o}}{\hbar^2} = \frac{\mathcal{A}^{5/3}}{68.4}\ \text{MeV}^{-1}. \tag{14}$$

This result is close to what one would obtain for a sharp-edged liquid drop (see, e.g., Ref. [24]). One would get from this reference, with a radius parameter $r_{\rm o} = 1.2049$ fm [25], a value for the rigid-body moment of inertia merely smaller by 2% with respect to our estimate.

Since for any reasonable value of the deformation parameter q the function $\Theta(q)$ is not too different from unity, one may conclude that the generalized moments of inertia A, B, and C are about equal. One has found in the explicit microscopic calculations of Ref. [15] that this is indeed the case (up to $\approx$10% in normally deformed and $\approx$15% in superdeformed nuclei).

To carry out the calculation of the generalized moments of inertia A, B, and C we need to know the deformation parameter q. It can be determined from the mass quadrupole moment which can be quite accurately approximated, for a compact deformed nuclear shape, using an ellipsoidal shape ansatz, by (see Ref. [24])

$$Q(q) = \tfrac{2}{5}\mathcal{A}^{5/3} r_{\rm o}^2 q^{-2/3}(q^2 - 1), \tag{15}$$

where again $r_{\rm o} = 1.2049$ fm. Taking, when available, the experimental intrinsic charge quadrupole moment $Q_{\rm ch}$ from Ref. [26], deduced from $B(E2)$ data, and using the approximate scaling relation

$$Q = \frac{\mathcal{A}}{Z} Q_{\rm ch}, \tag{16}$$

the deformation parameter q can then be fixed such that Eq. (15) yields the experimental mass quadrupole moment. Knowing q, the generalized moments of inertia A, B, and C are determined through Eqs. (6) and (13), and the total excitation energy $E(\Omega)$ is given through Eq. (5). Whenever no data for $Q_{\rm ch}$ could be found in Ref. [26], we have deduced the corresponding charge quadrupole moments from calculated values of the usual axial quadrupole deformation parameter β obtained in the theoretical systematic study of Ref. [27]. In this case the charge quadrupole moment $Q_{\rm ch}$ is evaluated from β according to the crude lowest-order expression

$$Q_{\rm ch} = \frac{3Zr_0^2\mathcal{A}^{2/3}}{\sqrt{5\pi}}\beta \approx 1.09Z\mathcal{A}^{2/3}\beta(\text{fm}^2). \tag{17}$$

III. DETERMINATION OF MODEL PARAMETERS

The generalized moments of inertia A, B, and C being known, there are two parameters, a global scale parameter k and a critical angular velocity Ω_c, whose values should be determined in order to compute the rotational energy as a function of the given Ω values through Eq. (5).

A. Critical angular velocity

According to the model presented in Ref. [15], upon which the present approach is based, we have at first related $E_c^{\rm rot}$ to a rough estimate of $E_{\rm o}$ according to

$$E_c^{\rm rot} = \tfrac{1}{2}\mathcal{J}_c\Omega_c^2 = 2E_{\rm o}. \tag{18}$$

This way to define the critical angular velocity Ω_c is similar to what is done in the theory of type-I superconductivity (to define the critical magnetic field) [28,29]. One remark should be made, however, about the factor of two appearing here between the two energies $E_c^{\rm rot}$ and $E_{\rm o}$, which is at variance with what is found in the magnetic-dipole case. It comes from the fact (see the proof in Ref. [15]) that we do not have the same dipole-dipole-type interaction energy as in magnetism since in our case the stable configuration corresponds to an anti-alignment.

As for the specific value of $E_{\rm o}$ we note that the correlation energy, which is the gain in binding energy in going from a noncorrelated solution to a correlated one, has been roughly estimated in Ref. [30] to be equal to 2.3 MeV on average over the whole nuclear chart. As it appears from explicit calculations performed in Ref. [15] with the SkM* interaction [22], the ratio of the pair condensation energy to the corresponding correlation energy is found to be approximately two. This estimate (see the discussion in Appendix A of Ref. [15] and its Fig. 8 in particular) has been deduced from explicit calculations conserving exactly the particle numbers (within the so-called highly truncated diagonalization approach of Ref. [31]). The rough

constancy and particular value of the ratio of condensation and correlation energies have been demonstrated for a very wide range of residual interaction strengths and a sample of realistic single-particle energy spectra of normal-deformed and superdeformed states of heavy nuclei. On this basis we will therefore take here a value of $E_{\rm o} = 4.6$MeV.

To determine the critical angular velocity Ω_c at which pairing correlations are going to vanish, one can, following Eq. (18), thus write

$$\Omega_c^2 = \frac{4E_{\rm o}}{\mathcal{J}_R}. \tag{19}$$

As discussed in Appendix A, the results obtained using the above definition of Ω_c leave ample room for improvement. Consequently, we have removed the too-crude ansatz of a constant value for $E_{\rm o}$ and investigated a simple yet sufficiently efficient dependence of $E_{\rm o}$ on the numbers of neutrons and protons (N and Z). For that purpose, we have defined an energy indicator reflecting the intensities of pairing correlations for a given even-even nucleus. With a two-body $|T_z| = 1$ residual interaction and limiting particle-hole excitations to pair transfers, one knows [32] that the proton and neutron wave functions are factorizable. Therefore, the strength of the pairing regime is essentially reflecting the values of averaged single-particle (s.p.) neutron and proton level densities at the Fermi surface. Yet a difficulty arises from the fact that these level densities are *a priori* different for neutrons and protons. It is therefore necessary within our simple approach to combine information on these level densities for both charge states.

To quantify the strength of the neutron and proton pairing correlations for a given nucleus defined by its nucleon numbers (N, Z), we have chosen to consider the experimental three-point mass differences [33] for adjacent nuclei in the isotopic (for neutrons) and isotonic (for proton) relevant series. These differences $\Delta_q^{(3)}(N, Z)$ are defined, for instance for neutrons, through the binding energies E or the neutron-separation energies S_n by

$$\begin{aligned}\Delta_n^{(3)}(N, Z) &= \frac{(-)^N}{2}[E(N-1, Z) + E(N+1, Z) - 2E(N, Z)] \\ &= \frac{(-)^N}{2}[S_n(N+1, Z) - S_n(N, Z)].\end{aligned} \tag{20}$$

To avoid spurious (for our purpose) mean-field effects due to the quantization of s.p. energies (see, e.g., Ref. [34]) we have not considered these differences for the even-even (N, Z) nuclei under study but the averaged differences for the $(N-1, Z)$ and $(N+1, Z)$ nuclei in the neutron case and for the $(N, Z-1)$ and $(N, Z+1)$ nuclei for protons. What remains is essentially due to the breaking of one pair, upon considering the ground state of odd-nuclei as seniority one states and assuming a type of Koopmans approximation. It is worth noting, as demonstrated in Ref. [35], that these three-point mass differences are not free from some small errors due to polarization effects, as compared with direct microscopic calculations of masses. Yet, it is our contention that, for our model approach, the quantities

$$\Delta_n = \tfrac{1}{2}\big[\Delta_n^{(3)}(N-1, Z) + \Delta_n^{(3)}(N+1, Z)\big], \tag{21}$$

$$\Delta_p = \tfrac{1}{2}\big[\Delta_p^{(3)}(N, Z-1) + \Delta_p^{(3)}(N, Z+1)\big], \tag{22}$$

provide a sufficient knowledge of the pairing gaps for neutrons and protons. This is all more so that, as we will see, we will have to make a global (i.e., for all considered nuclei) normalization of the retained pairing energy indicator so that only their relative variations is of relevance for us.

The precise definition of the above-mentioned pairing energy indicator is as such

$$Y_{\rm pair} = \sqrt{\Delta_n^2 + \Delta_p^2}, \tag{23}$$

where Δ_n and Δ_p are defined for an (N, Z) even-even nucleus as given in Eqs. (21) and (22).

The gap dependence retained for $Y_{\rm pair}$ comes from the pair condensation energy in a crude seniority force model which varies as the square of the gap assuming the same value for the model pairing matrix element (the same holds for all nuclei considered and the two charge states).

Then we reformulate Eq. (19) by defining the critical angular velocity as

$$\Omega_c^2 = \alpha \frac{4E_{\rm o}}{\mathcal{J}_c}, \tag{24}$$

introducing a factor α which will take care of the dependence of the critical angular velocity Ω_c on $Y_{\rm pair}$.

We have tested three different versions of our approach, where the critical rotational energy defined through Ω_c is not dependent on the ground-state pairing correlations (version 1), where this dependence is linear in the energy $Y_{\rm pair}$ (version 2), and where it is inversely proportional to $Y_{\rm pair}$ (version 3), thus defining

$$\text{version 1} : \alpha = 1, \tag{25}$$

$$\text{version 2} : \alpha = \frac{Y_{\rm pair}}{Y_{\rm pair}^0}, \tag{26}$$

$$\text{version 3} : \alpha = \frac{Y_{\rm pair}^0}{Y_{\rm pair}}, \tag{27}$$

where $Y_{\rm pair}^0$ has been determined empirically, as discussed in Appendix A.

From the study performed in Appendix A, one finds that the third version, Eq. (27), is by far to be preferred with a value of $Y_{\rm pair}^0$ equal to about 0.85 MeV (note that this specific value is contingent upon the choice of $E_{\rm o}$ from the estimated value of Ref. [30]). This is illustrated in Figs. 1 and 2 and discussed in Appendix A.

In other words, it appears that the disappearance of pairing due to the rotational mode seems to be all the more rapid given that there are more correlations at zero spin. This somewhat counterintuitive result is confirmed qualitatively by the results of explicit microscopic calculations of the function $\omega(\Omega)$ performed in Ref. [15]. There, for the two well-deformed ^{154}Sm and ^{178}Hf nuclei corresponding respectively to $Y_{\rm pair}$ values of 1.108 and 0.893 MeV, one has found $\hbar\Omega_c$ values of about 0.3 and 0.4 MeV, respectively, confirming thus the above discussed trend.

A tentative explanation for that could be proposed in terms of the well-known phase opposition for the variation of the

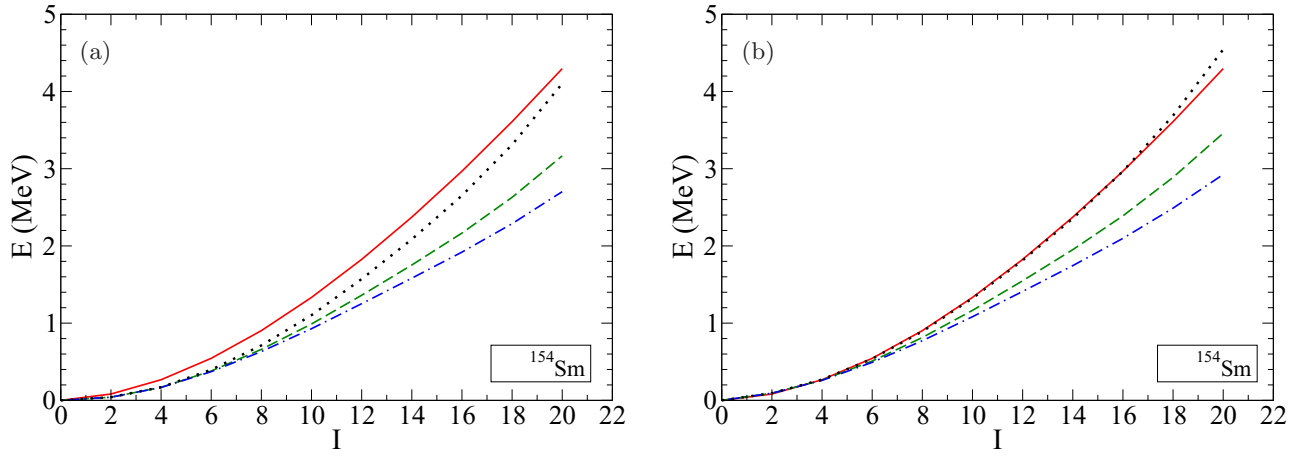

FIG. 1. Comparison between the experimental $E(I)$ (red solid line) and the theoretical curves obtained using two different ways to determine the rotational angular velocity Ω that enters Eq. (5): (a) using Ω_a, Eq. (A4) and (b) using Ω_b, Eq. (A6). The three theoretical curves shown in each of these plots are obtained with different Ω_c values corresponding to version 1 (green dashed), version 2 (blue dashed-dotted), and version 3 (black dotted line).

absolute values of the shell effect and pair condensation energies. A minimum of the former corresponds to a maximum of the latter upon varying some continuous variable as nuclear deformation, and vice versa. This is clear from the consideration of s.p. level density at the Fermi surface. Now, as analyzed for instance in Ref. [36], shell effects perturb the patterns of current densities whose flows lose their smooth character. They are thus likely to create a deficit of the Coriolis antipairing effect with respect to an average behavior represented by the approach followed in version 1.

B. Determination of the scale factor *k*

The next crucial point is to build up a reliable determination of the constant k appearing in Eq. (3) and, consequently, in Eq. (5).

To do so, we place ourselves in the adiabatic limit. Consequently, we consider the state with the lowest nonvanishing experimentally available collective velocity, namely, the first member (2^+) of the rotational band. Specifically, in what follows, we discuss two possible ways to obtain the k parameter value.

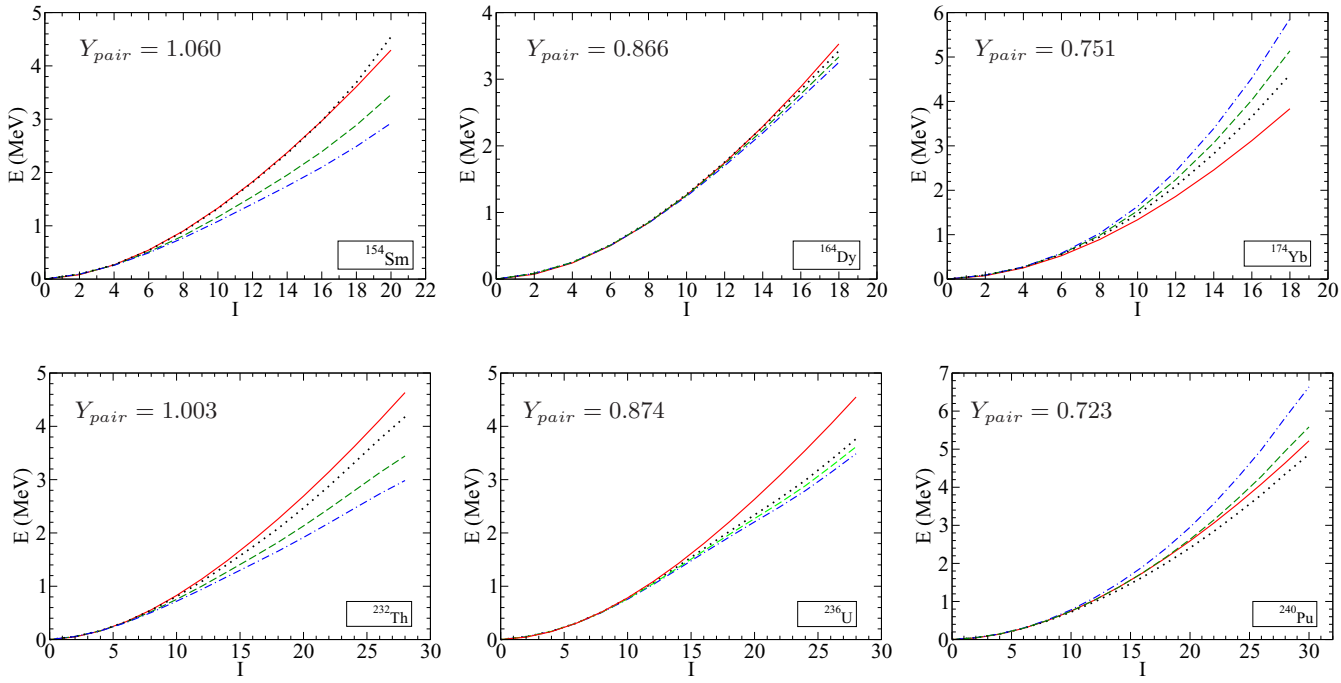

FIG. 2. Comparison between the experimental rotational energy $E(I)$ (red solid line) and the model prediction obtained through Eq. (5) with the angular velocity Ω_b of Eq. (A6) for the different α values determining the impact of the pairing correlations on the value of the critical angular velocity Ω_c as already applied in Fig. 1. The corresponding pairing-correlation indicators $Y_{\rm pair}$ (in MeV^2) are also reported.

As a first approach one takes for mere input the energy $E(2^+)$ of the 2^+ state:

$$E(2^+) = \frac{1}{2}\frac{6\hbar^2}{\mathcal{J}_2}, \tag{28}$$

defining a moment of inertia $\mathcal{J}_2$ for this 2^+ state. Together with using another expression for the $E(2^+)$ energy,

$$E(2^+) = \frac{\mathcal{J}_2}{2}\Omega_2^2, \tag{29}$$

one gets the angular velocity Ω_2 that enters Eq. (5).

Using Eq. (29) together with Eq. (5), one obtains for the moment of inertia $\mathcal{J}_2$,

$$\mathcal{J}_2 = Ak^2\left(1-\xi_2^2\right)^2 - 2Bk\left(1-\xi_2^2\right) + C, \tag{30}$$

where ξ_2 has the value of $\xi = \Omega/\Omega_c$ corresponding to the 2^+ rotational state, which appears, in fact, to be a small quantity.

As mentioned above, $A \approx B \approx C$, and therefore $C - \mathcal{J}_2 < B$. Thus one obtains two distinct real solutions of Eq. (30). Out of these two solutions, since for obvious physical reasons k should be smaller than 1, we unambiguously retain the solution

$$k = \frac{B}{A\left(1-\xi_2^2\right)}\left[1 - \sqrt{1 - \frac{A(C-\mathcal{J}_2)}{B^2}}\right]. \tag{31}$$

There is another possible version of the same approach (i.e., relying on the same input, namely, implying merely the energy of the 2^+ state) which consists in finding both the constant k and the angular velocity Ω_2 leading to the desired spin (evaluated according to the method which will be described in Sec. 4) and energy of the 2^+ state by solving a system of coupled linear equations. It is presented in some detail in Appendix B. It yields, as it turns out, k values that are identical to those obtained through Eq. (31) by a fraction of a percent for all nuclei investigated in the present study. The difference in the two k values is generally rather of the order of 10^{-5} for a k value of about 0.3. This results in energy differences of the order of a few keV in the worst case for the highest angular-momentum values ($E > 10$ MeV), but is most of the time much better [$\Delta E = 10$ eV in ^{154}Sm ($I = 22$) and $\Delta E = 121$ eV in ^{240}Pu ($I = 32$)].

IV. DETERMINATION OF THE ANGULAR VELOCITY ASSOCIATED WITH A GIVEN SPIN

We now use the dynamical model underlying our approach to determine theoretically from our energy function the value of the angular velocity $\Omega(I)$ corresponding to a given state I^+ of the rotational band.

The above theoretical developments based on classical-physics concepts and leading to the polynomial expression of $E(\Omega)$ in Eq. (5) involve the norm of the angular momentum. It is given (in units of $\hbar$), by $\tilde{I} = \sqrt{I(I+1)}$ as defined in Eq. (A1). Consequently we will use $\tilde{I}$ instead of I in all relevant equations.

As discussed above, in a semiquantal Routhian approach, $\hbar\Omega$ is the Lagrange parameter associated with a constraint on the value of $\tilde{I}$, such that

$$d\tilde{I} = \frac{1}{\hbar}\frac{dE}{\Omega} \text{ resulting in } \tilde{I}(\Omega) = \int_0^{\Omega} \frac{1}{\hbar\Omega'}\frac{dE}{d\Omega'}d\Omega' \tag{32}$$

and using the derivative $dE/d\Omega$ given by

$$\frac{dE}{d\Omega} = \{[C - 2Bk + Ak^2] + 4[Bk - Ak^2]\xi^2 + 3Ak^2\xi^4\}\Omega, \tag{33}$$

one obtains

$$\hbar\tilde{I}(\Omega) = \left\{[C - 2Bk + Ak^2] + \tfrac{4}{3}[Bk - Ak^2]\xi^2 + \tfrac{3}{5}Ak^2\xi^4\right\}\Omega. \tag{34}$$

With typical values for the parameter k ($k \approx 0.3$) and remembering that the generalized moments of inertia are all about equal (with $B \leqslant A \leqslant C$) it turns out from

$$\hbar\frac{d\tilde{I}}{d\Omega} = [C - 2Bk + Ak^2] + 4[Bk - Ak^2]\xi^2 + 3Ak^2\xi^4 \tag{35}$$

that $d\tilde{I}/d\Omega$ is positive definite and thus $\tilde{I}(\Omega)$ is a monotonically increasing function. It can, therefore, be unambiguously inverted to obtain Ω as a function of the angular-momentum quantum number I of the state to be considered.

V. PRESENTATION AND DISCUSSION OF THE RESULTS

Calculations of the energies of the entire rotational band as a function of the angular momentum $\hbar I$ have been performed for a selection of 14 rare-earth and 10 actinide nuclei. They have been compared with available experimental data [33].

To put in perspective the choice of nuclei which has been made, let us mention that, in the region defined by $50 \leqslant Z \leqslant 82$ and $82 \leqslant N \leqslant 126$, there are 58 even-even experimentally studied nuclei whose energy ratio R_{42} of the first two members of the ground-state band are larger than three and, correspondingly, there are 31 in the $Z \geqslant 82$ and $82 \leqslant N \geqslant 126$ region. Out of those we chose at least one isotope per element under the following constraints:

(1) the existence of a sufficiently long known yrast line sequence (typically up to $20\hbar$ or possibly much higher);
(2) good rotor properties as measured by the ratio $R_{42} \geqslant 3.1$;
(3) the possibility of determining with sufficient accuracy the odd-even mass differences (a possibility thus ultimately related with the accuracy of the relevant mass measurements).

Moreover, we have included short isotopic series in the middle of each of the regions considered (namely, seven erbium and four plutonium isotopes).

In addition to the pairing indicators Δ_n and Δ_p discussed in Sec. III A, Eqs. (21) and (21), we have reported in Tables I and II, for each of the 24 nuclei retained for the discussion, the quantities which enter the definition of the polynomial expression of $E(\Omega)$, namely, the experimental 2^+ energies [33] and the charge quadrupole moments (from Refs. [26] or [27]) as specified in Sec. II B.

In Figs. 3 and 4 we compare the experimental energy curves as functions of the angular-momentum quantum

TABLE I. Experimental charge quadrupole moments [26] Q_{ch} (in fm^2), energies of the first 2^+ excited state (in keV), energy ratio of second- to first-excited state of the rotational band, together with averaged neutron gap Δ_n and proton gap Δ_p (in keV) obtained from three-point odd-even mass differences for a series of rare-earth nuclei. Charge quadrupole moments quoted with * are taken from the theoretical results of Ref. [27] (see text). All reported energies are taken or deduced from the data of Ref. [33].

Nucleus	Q_{ch}	E_{2^+}	E_{4^+}/E_{2^+}	Δ_n	Δ_p
$^{152}_{60}$Nd	649	72.4	3.267	816	677
$^{154}_{62}$Sm	662	82.3	3.242	885	666
$^{156}_{64}$Gd	683	89.2	3.239	919	692
$^{164}_{66}$Dy	750	73.4	3.300	679	538
$^{160}_{68}$Er	663	125.8	3.099	1061	979
$^{162}_{68}$Er	710	102.1	3.230	985	877
$^{164}_{68}$Er	740	91.4	3.277	943	762
$^{166}_{68}$Er	766	80.6	3.289	791	623
$^{168}_{68}$Er	763	79.8	3.309	648	554
$^{170}_{68}$Er	765	78.6	3.309	604	503
$^{172}_{68}$Er	768*	77.0	3.315	579	531
$^{174}_{70}$Yb	773	76.5	3.309	535	528
$^{170}_{72}$Hf	730	100.8	3.195	993	895
$^{178}_{74}$W	791*	105.9	3.236	776	791

number I with our theoretical predictions for our sample of rare-earth (Fig. 3) and actinide (Fig. 4) nuclei. Reported experimental energies correspond to the yrast bands. The theoretical energies have been calculated through the polynomial expression $E(\Omega)$, where the angular velocity for a given value of I is obtained as the solution of the implicit equation (34). The agreement between the two energy curves is generally good up to moderate spins ($\approx 12\hbar$) and in many cases amazingly good up to very high spins (e.g., in ^{154}Sm, ^{164}Dy, ^{230}Th, and ^{242}Pu). There are also cases where a clear disagreement appears, which will be discussed later, in particular in the context of band crossings.

On these figures we have also reported, for all nuclei, energy curves where the angular velocities entering Eq. (5) have been deduced from the experimental spectra by averaging what is deduced from the two gamma transition energies feeding and depopulating the considered band state according to Eq. (A6), in the same way as done in Figs. 5 and 6.

TABLE II. Same as Table I but for a series of actinide nuclei.

Nucleus	Q_{ch}	E_{2^+}	$E_{4^+/2^+}$	Δ_n	Δ_p
$^{230}_{90}$Th	899	53.2	3.271	715	739
$^{232}_{90}$Th	966	49.4	3.284	682	737
$^{234}_{92}$U	1035	43.5	3.296	584	606
$^{236}_{92}$U	1080	45.2	3.304	570	663
$^{236}_{94}$Pu	1092*	44.6	3.304	559	460
$^{238}_{94}$Pu	1126	44.1	3.312	502	508
$^{240}_{94}$Pu	1144	42.8	3.309	489	534
$^{242}_{94}$Pu	1161	44.5	3.307	514	568
$^{246}_{96}$Cm	1226	42.9	3.314	500	625
$^{248}_{96}$Cm	1228	43.4	3.313	545	665

It is significant to note that, even though one has incorporated much more data (energies at all spin values) in the calculated (dash-dotted) curves using the so-called experimental Ω value as defined by Eq. (A6), they fail to reproduce the observed spectra in a better way than our theoretical approach (dotted curves), relying on the inversion of Eq. (34), and which includes merely the energy of the first member of the band. Clearly, the former set of experimental Ω values encompasses more dynamical effects than our model can describe. It is therefore not too surprising that they are unfit to reproduce within our model the observed trends whenever physical effects other than those included in this model are at work.

In particular, when a marked backbending is present (as, e.g., in ^{160}Er) after the crossing of the s and g bands, the variation with I of the yrast band energies is clearly too fast. Indeed, our model applies spuriously to s-band states the variation which has been defined in the g band. The calculated trend is thus easily explained since, due to the Pauli-pairing blocking, all things being kept equal except the pairing correlations, the moments of inertia of the s band are larger than those of the g band.

A finer assessment of the behavior of energies within a rotational spectrum is obtained when considering quantities which are related to a first-order derivative of the energy with respect to the angular momentum, namely, the so-called kinematical moments of inertia $J^{(1)}$. This quantity divided by $\hbar^2$ is defined microscopically as the polarizability associated, in the Routhian approach, with the constraint on $\tilde{I}$ where the Lagrange multiplier is $\hbar\Omega$. One then has

$$\frac{J^{(1)}}{\hbar^2} = \frac{\tilde{I}}{\hbar\Omega}. \tag{36}$$

To determine $J^{(1)}$ one thus needs the values of Ω associated with each considered state. Here we chose to extract them from the spectra by using Eq. (A4). From this, one gets the corresponding kinematical moment of inertia as

$$\frac{J^{(1)}}{\hbar^2} = \frac{\tilde{I}_{av}}{\hbar\Omega} = \frac{2I-1}{E_{I\to I-2}}. \tag{37}$$

Incidentally, one notes that such a definition of the moments of inertia is consistent with the one used for $I = 2$ in Sec. III B to evaluate the values of the model parameter k. We have seen above that a one-sided derivative to define the angular velocity (26) is not such an optimal choice. Indeed, extracting the Ω values from the spectra upon using the double-sided derivative leading to Eq. (28) turns out to be more appropriate, as demonstrated there. This is also substantiated in Appendix C. We nevertheless keep this definition (37) of $J^{(1)}$ to be consistent with what is done in the experimental analysis, see, e.g., Ref. [37]. Indeed, for the comparative numerical test between the experimental data and the corresponding theoretical predictions of the series of

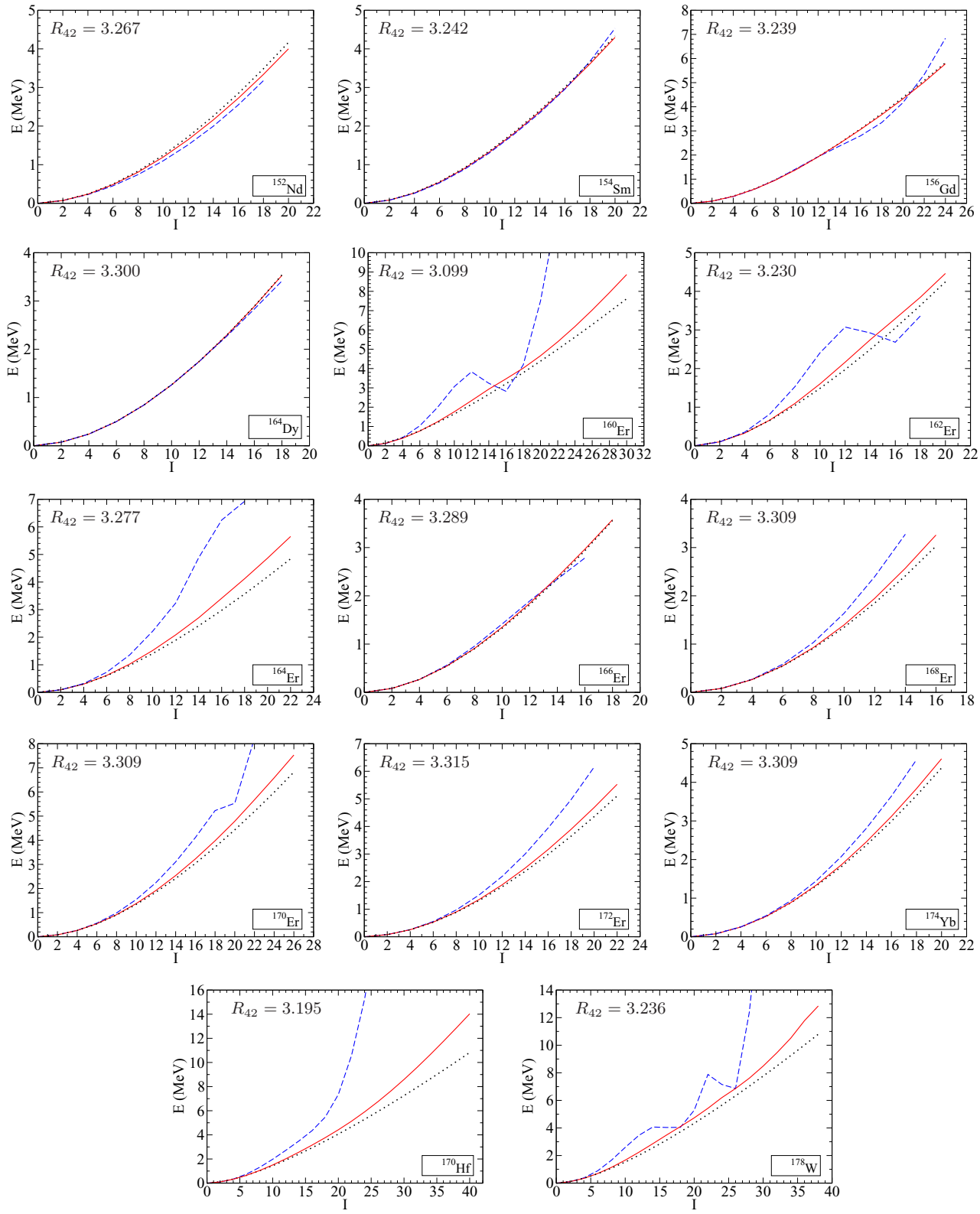

FIG. 3. Comparison of experimental [33] and theoretical rotational energies as a function of the quantum number I for fourteen rare-earth nuclei. The experimental energy curves (red solid) are reported alongside with those of our model (black dotted) and those (blue dashed) where the Ω values are defined from the experimental spectra as discussed in the text. The ratios R_{42} of the energies of the first-excited members of the band are also reported.

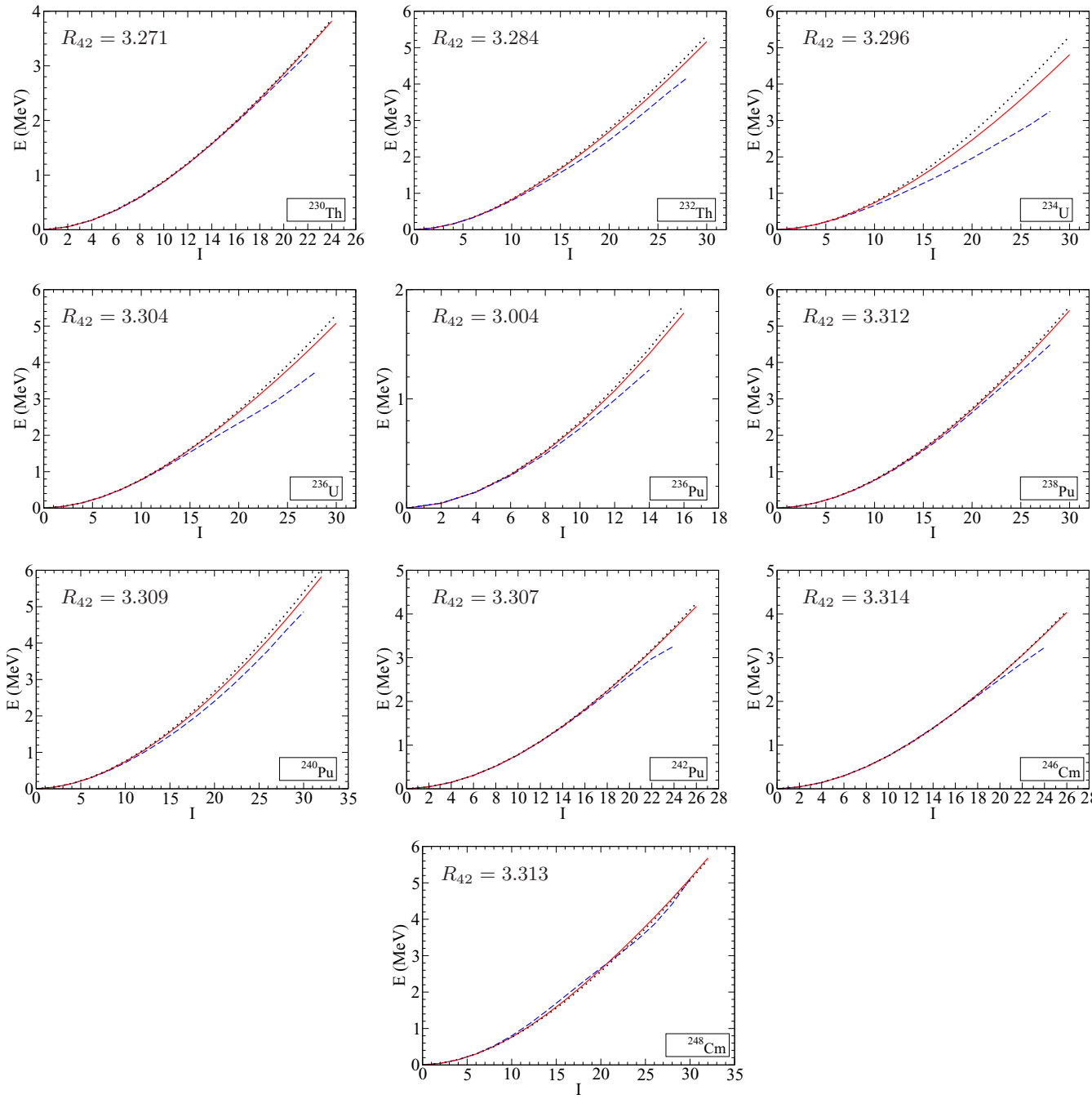

FIG. 4. Same as Fig. 3 but for ten actinide nuclei.

rotational energies as functions of I, only the consistency of both methods counts.

In Figs. 5 and 6 we present for the 24 considered nuclei the variation of the kinematical moments of inertia $J^{(1)}$ as functions of Ω^2, comparing the experimental trends with our model estimates.

Let us first discuss the results obtained for rare-earth nuclei as displayed in Fig. 5. As is well known (see, e.g., Ref. [38]), many nuclei of this region present a backbending pattern due (at least for the first backbending) to an alignment of deformed single-particle states stemming from the intruder neutron $1i13/2$ spherical orbital. This is clearly the case for the ^{160,162,164}Er and ^{178}W nuclei and is only suggested in the less clean-cut cases of ^{156}Gd, ^{170}Er, and ^{170}Hf. It is clear that our model cannot reproduce this highly noncollective phenomenon. On the other hand, the behavior of the kinematical moment of inertia of the g band is reasonably well reproduced in our model for these nuclei. In some other nuclei (^{152}Nd, ^{154}Sm, and ^{164}Dy) the model is in quite good agreement over all of the experimentally known yrast bands. For three nuclei (^{168}Er, ^{172}Er, and ^{174}Yb), the almost linear behavior (in Ω^2) of the data is reproduced by our model, but not the slope.

The situation is much more satisfactory in actinide nuclei (Fig. 6). As often remarked (see, e.g., Ref. [37]) deformed

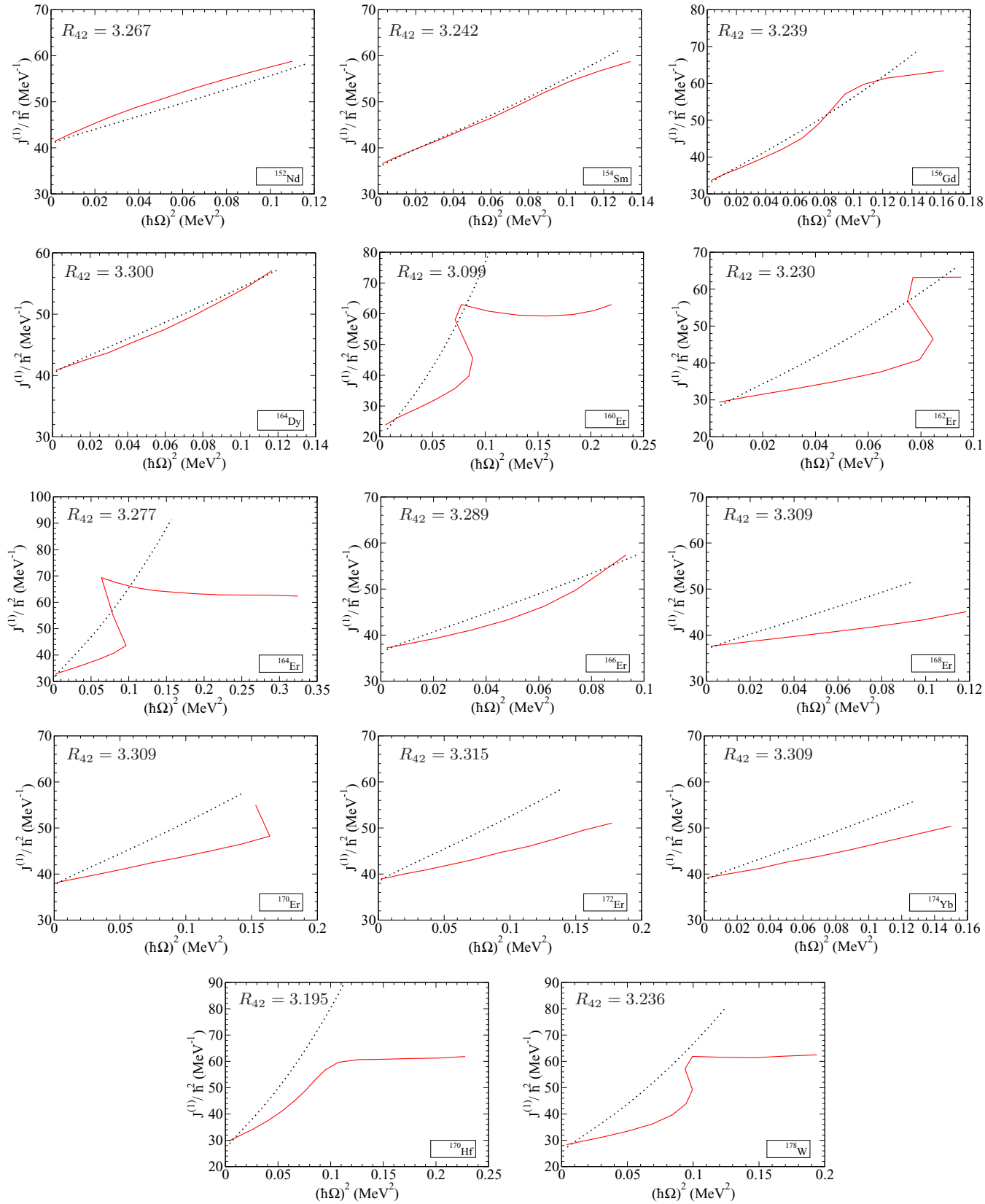

FIG. 5. Comparison between theoretical (black dotted) and experimental (red solid lines) values for the kinematical moment of inertia $\mathcal{J}^{(1)}$ as a function of the angular frequency squared Ω^2 for fourteen rare-earth nuclei. The ratios R_{42} of the energies of the first-excited members of the band are also reported.

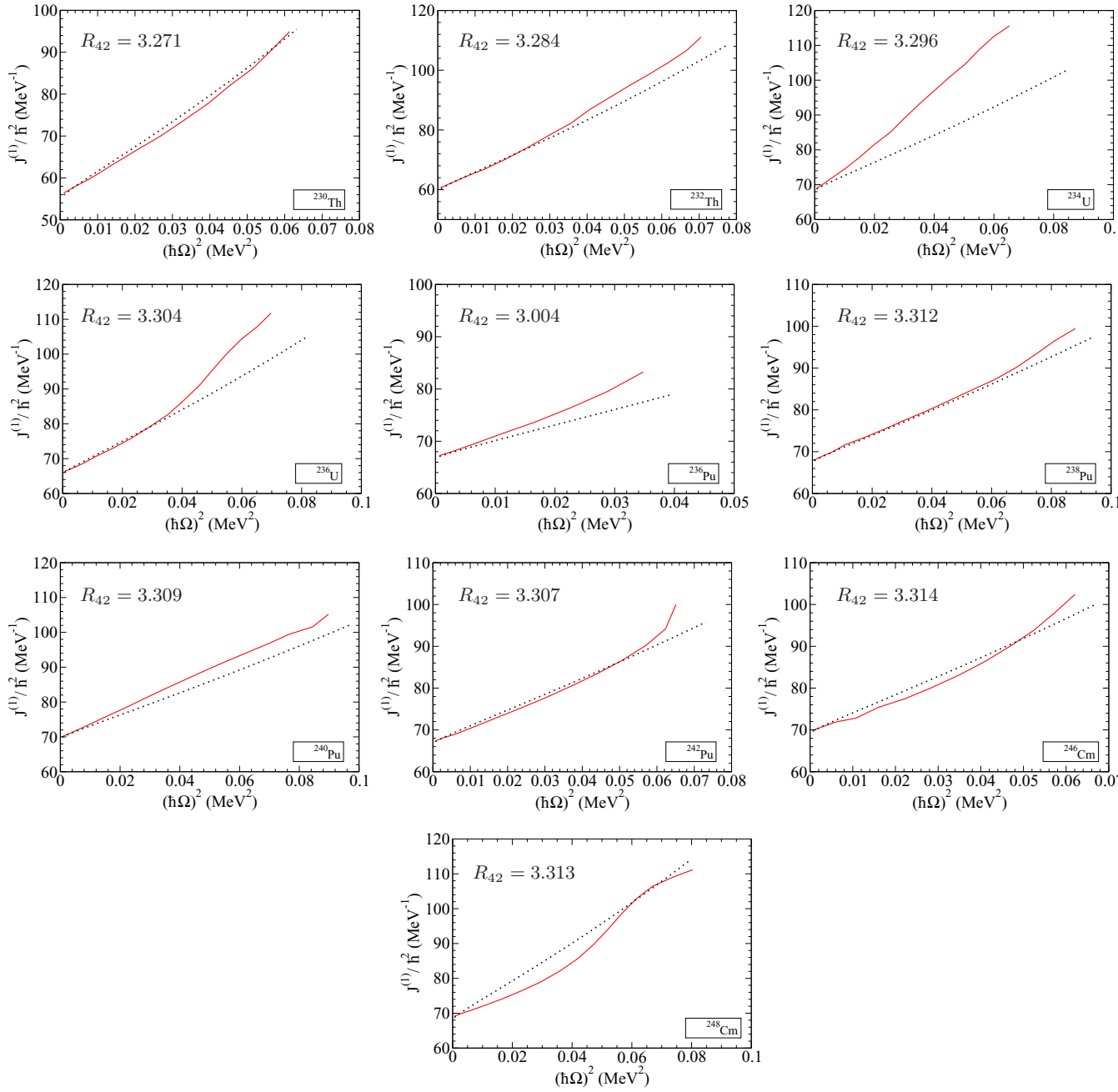

FIG. 6. Same as Fig. 5 but for ten actinide nuclei.

nuclei are better rotors than what is observed in the rare-earth region. Here all calculated nuclei exhibit a ratio $R_{42} \geqslant 3.30$, apart from the two thorium isotopes considered (^{230}Th and ^{232}Th) where this ratio is still rather high (3.27 and 3.28). With only one exception (^{234}U), all nuclei present a trend of $J^{(1)}(\Omega^2)$ in good (and sometimes excellent) agreement with the data. In some cases though, some new physics appears at moderately high angular-momentum values (as in the clear examples of ^{236}U and ^{238,242}Pu nuclei).

As it appears from all the theoretical curves of Figs. 5 and 6, one obtains an almost linear variation of $J^{(1)}$ as a function of Ω^2. As clearly seen from Eq. (34), the model kinematical moment of inertia is a polynomial of degree two in Ω^2. The above-quoted results reflect eloquently that the terms in Ω^4 in the kind of Harris expansion resulting from our approach are almost negligible. In other words, the Coriolis antipairing effect which is modeled here practically does not generate terms of order higher than two in the expression of the kinematical moment of inertia as a function of Ω.

As said in the introduction, a simple phenomenological parametrization of both the dependence of the moment of inertia and of the correlation energy on the pairing gap has been proposed by the authors of Refs. [12,13]. An *a priori* improved version has been later presented [14]. It makes use

for each nucleus of similar data as made in our paper (calculated BCS gaps and rigid-body moments of inertia as well as first 2^+ excitation energies). Through a minimization of the total (correlation plus collective rotational) energy for each angular momentum, they produce rotational spectra. Upon comparing our results with theirs as displayed in Ref. [14], it turns out that our present approach reproduces, on average, the experimental data better but only to a small extent. If our goal would have been merely to reproduce experimental results, one would certainly recommend the use of the very efficient parametrizations of Refs. [12–14]. But what we here aim at is not only that but also to validate a collective model of coupled currents to assess some physical ideas at the core of the CAP approach.

VI. CONCLUSIONS

As is well known [11], the collective quenching of pairing correlations due to a global rotational motion may be described as the appearance in the correlated solutions of intrinsic vortical modes. It had been shown [15] that the corresponding currents can be well described quantitatively within the framework of Chandrasekhar's S-ellipsoid linear velocity fields [16]. We have presented a model based on this conjecture leading, for even-even nuclei, to a Harris-type expansion of the rotational energy $E(\Omega)$ (up to cubic terms in Ω^2), where Ω is the angular velocity of global rotation.

The coefficients of such an expansion do not result from a trivial fit of $E(\Omega)$ but are deduced from three pieces of experimental data pertaining to the properties of the first two states (0^+ and 2^+) of each rotational band (pairing correlations content in neighboring nuclei from mass measurements, intrinsic charge quadrupole moment from $B(E2, 2^+ \rightarrow 0^+)$ data and the excitation energy of the first 2^+ state).

In spite of the fact that the input data used in our approach are exclusively pertaining to the ground state and the energy of the first-excited state of the rotational band, the resulting agreement with measured rotational band energies is found to be excellent up to very high spins ($\approx 30\hbar$) in many deformed rare-earth and actinide nuclei. Taking into account the model assumptions, such an agreement, when obtained, provides a reasonable ground for describing the collective behavior merely in terms of the collective coupling of rotation and pairing correlations.

Clearly, the model presented here does not replace currently available fast and realistic microscopic Routhian calculations within the Hartree-Fock-Bogoliubov approximation or a relativistic mean field plus pairing approach (for a brief survey, see, e.g., the Sec. VI F.1 in Ref. [39]). Our aim, as already stated, is merely to provide a quantitative assessment of the S-ellipsoid model coupling intrinsic and global collective rotational currents yielding the CAP quenching of pairing correlations. As is well known, other physical effects either of a collective nature (such as, e.g., centrifugal stretching) or pertaining to single (quasi-)particle degrees of freedom (such as, e.g., particle alignment) are to be considered. It is our contention that our model, beyond its successful illustration of the CAP hypothesis, provides a useful baseline to visualize, upon increasing the angular velocity, where and how much these other modes are playing a significant role.

ACKNOWLEDGMENTS

One of the authors (P.Q.) gratefully acknowledges the hospitality extended to him by the IPHC Strasbourg during his numerous visits.

APPENDIX A: DEPENDENCE OF THE CRITICAL ANGULAR MOMENTUM Ω_c ON THE LEVEL OF PAIRING CORRELATIONS

To determine which version of the $Y_{\rm pair}$ dependence of Ω_c, defined in Eqs. (25–27), gives a better account of the experimental data, we have performed indicative calculations for a sample of nuclei taken from the two regions of interest (well-deformed rare-earth and actinide nuclei). For these nuclei we have calculated the values of the polynomial expression of $E(\Omega)$, Eq. (5), in the above three versions with a parameter k determined according to the method detailed in the next section. In these preliminary calculations the angular velocities Ω have been determined for each state of the band from the experimental transition energies.

There are, as a matter of fact, several different ways to extract the angular velocities Ω from the rotational band energies. All of them are grounded, however, on the fact that, in a Routhian-type variational calculation, one searches to determine the energy of the nuclear system under the constraint of a given value of the modulus of the angular-momentum operator $\hat{I}$ (divided by $\hbar$), which is defined as

$$\tilde{I} = \frac{\sqrt{\langle \hat{I}^2 \rangle}}{\hbar} = \sqrt{I(I+1)}. \tag{A1}$$

The Lagrange multiplier associated with this constraint on $\tilde{I}$ is $\hbar\Omega$ and is obtained, as is well known, as the derivative of the quantity to be varied (the energy E) with respect to the value of the quantity which is constrained, namely $\tilde{I}$:

$$\hbar\Omega = \frac{dE}{d\tilde{I}}. \tag{A2}$$

To deduce Ω in practice from a discrete spectrum (experimental or theoretical), one has thus to evaluate the above derivative in some approximative way, consisting all in some discretization procedure. Here we consider two possibilities.

(a) One proceeds as currently done in the experimental analysis (see, e.g., Ref. [37]) by considering only the transition depopulating the considered state labeled by the quantum number I (namely, $E_{I\rightarrow I-2}$). This defines an angular velocity denoted as $\Omega_{\downarrow}$. The angular momentum where the above derivative is evaluated is taken at the median energy between the states defined by I and $I-2$, corresponding thus to

$$\tilde{I} = \tilde{I}_{av} = \sqrt{I^2 - I + 1}.$$

The resulting variation is thus given in general by

$$\Delta\tilde{I} = \frac{2I-1}{\tilde{I_{av}}}\frac{\Delta I}{2}, \tag{A3}$$

and since $\Delta I = 2$ in this case, one obtains

$$\hbar\Omega_a = \hbar\Omega_\downarrow = \frac{\sqrt{I^2 - I + 1}}{2I - 1} E_{I\to I-2}. \tag{A4}$$

This procedure has the advantage that a value for Ω can be associated with every rotational state (even without knowing the energy of the populating state).

(b) Such a *one-sided* derivative could be quite inaccurate in the case of a fast variation of the rotational energy $E(I)$ with respect to the angular velocity. One could then think of using instead a combination of the Ω values obtained from derivatives corresponding to transitions depopulating and populating a given state. The value $\Omega_\uparrow$ of Ω obtained as in Eq. (A4) but for the populating state defined by $I + 2$ is

$$\hbar\Omega_\uparrow = \frac{\sqrt{I^2 + 3I + 3}}{2I + 3} E_{I+2\to I}. \tag{A5}$$

Thus, combining now the Ω values coming from the transition from above and the transition to below, one can define an angular velocity Ω_b as the mean value between $\Omega_\uparrow$ and $\Omega_\downarrow$, yielding

$$\hbar\Omega_b = \frac{1}{2}\left[\frac{\sqrt{I^2 + 3I + 3}}{2I + 3} E_{I+2\to I} + \frac{\sqrt{I^2 - I + 1}}{2I - 1} E_{I\to I-2}\right]. \tag{A6}$$

We present the results of such a preliminary study in two steps: First, we compare the experimental rotational energies [33] with the calculated energies for the three versions retained for the dependence of Ω_c on the pairing correlation content, through the definition of the α parameter, for a single nucleus, namely, ^{154}Sm, upon taking separately the experimental Ω values from Eqs. (A4) and (A6), respectively. From the results displayed in Fig. 1, one concludes first that version 3 of Eq. (27) to define the α parameter is to be preferred however Ω values are extracted. Furthermore, as could be expected, the definition of the experimental angular velocities upon using the information from both populating and depopulating transitions is far better than considering merely the data from the single depopulating transitions.

In a second step, we extend the above conclusion concerning the $Y_{\rm pair}$ dependence of Ω_c by considering a sample of six deformed nuclei taken from the rare-earth and actinide regions (^{154}Sm, ^{156}Dy, ^{174}Yb, ^{232}Th, ^{236}U, and ^{240}Pu). Here, we extract experimental Ω values by using merely the two-transition formula of Eq. (A6). As seen in Fig. 2, the conclusion drawn from the single case of ^{154}Sm is fully confirmed: the critical rotational energy should be preferably taken as inversely proportional to $Y_{\rm pair}$.

Let us mention sketchily now how we came to the retained value of $Y^0_{\rm pair}$. At first we have made calculations with $\alpha = 1$ (version 1). We noted that, in two cases, ^{156}Dy and ^{236}U corresponding to values of $Y_{\rm pair}$ close to a specific value $Y^0_{\rm pair} = 0.85$ MeV, namely, $Y_{\rm pair} = 0.866$ and 0.874 MeV, respectively, the theoretical and experimental energies coincide rather well, at least up to angular momenta $I \approxeq 12\hbar$. For nuclei whose $Y_{\rm pair}$ values are found far off these values, we remarked a rather systematic trend. For $Y_{\rm pair} > Y^0_{\rm pair}$, the calculated curves were found below the experimental curve, which is the case for ^{154}Sm and ^{232}Th (with $Y_{\rm pair} = 1.060$ and $Y_{\rm pair} = 1.003$ MeV^2, respectively). For $Y_{\rm pair} < Y^0_{\rm pair}$, the inverse trend is found, as seen for ^{174}Yb and ^{240}Pu (with $Y_{\rm pair} = 0.751$ and $Y_{\rm pair} = 0.723$ MeV, respectively). This has indeed led us to infer that the prescription of version 3 with the retained value of $Y^0_{\rm pair}$ should be best suited to take into account the impact of pairing correlations on the value of the critical angular velocity Ω_c.

APPENDIX B: RESOLUTION OF A SYSTEM OF COUPLED EQUATIONS TO DETERMINE THE CONSTANTS k AND Ω_2

One could propose the following procedure to adjust the constant k and the angular velocity Ω, which are the two quantities determining the rotational energy $E(\Omega)$, see Eq. (5), and the angular momentum $I(\Omega)$, see Eq. (34), in such a way that, for the 2^+ rotational state, the energy as well as the angular momentum are perfectly reproduced. This would mean that the constant k is no longer given by Eq. (31) but has to be iterated together with Ω so as to obtain the desired experimental values E^+_2 and $\tilde{I} = \sqrt{6}$.

Let us therefore start from Eqs. (5) which we rewrite now in the form

$$E(k,\Omega) = \frac{\Omega_c^2}{2}[C\xi^2 - 2Bk\xi^2(1-\xi^2) + Ak^2\xi^2(1-\xi^2)^2] \tag{B1}$$

and from the expression of $\tilde{I}(k,\Omega)$ given by Eq. (34).

Their partial derivatives with respect to k and Ω are

$$\frac{\partial E}{\partial k} = [Ak(1-\xi^2)^2 - B(1-\xi^2)]\Omega^2, \tag{B2}$$

$$\frac{\partial E}{\partial \Omega} = [C - 2Bk(1-2\xi^2) + Ak^2(1 - 4\xi^2 + 3\xi^4)]\Omega, \tag{B3}$$

and

$$\hbar\frac{\partial \tilde{I}}{\partial k} = \left\{2[Ak - B] + \frac{4}{3}[B - 2Ak]\xi^2 + \frac{6}{5}Ak\xi^4\right\}\Omega, \tag{B4}$$

$$\hbar\frac{\partial \tilde{I}}{\partial \Omega} = [C - 2Bk + Ak^2] + 4[Bk - Ak^2]\xi^2 + 3Ak^2\xi^4. \tag{B5}$$

To find iteratively the values of the two variables k and Ω that reproduce the experimental values for E^+_2 and $\tilde{I}$, we define the following dimensionless functions:

$$f(k,\Omega) = \frac{E(k,\Omega)}{E^+_2} - 1 \text{ and } g(k,\Omega) = \frac{\tilde{I}(k,\Omega)}{\sqrt{6}} - 1. \tag{B6}$$

One then attempts to minimize the function

$$S(k,\Omega) = f^2(k,\Omega) + g^2(k,\Omega) \tag{B7}$$

by the steepest descent method. The gradient of $S(k,\Omega)$ is

$$\vec{\nabla}S(k,\Omega) = \begin{pmatrix} 2\left[f(k,\Omega)\frac{\partial f}{\partial k} + g(k,\Omega)\frac{\partial g}{\partial k}\right] \\ 2\left[f(k,\Omega)\frac{\partial f}{\partial \Omega} + g(k,\Omega)\frac{\partial g}{\partial \Omega}\right] \end{pmatrix}. \tag{B8}$$

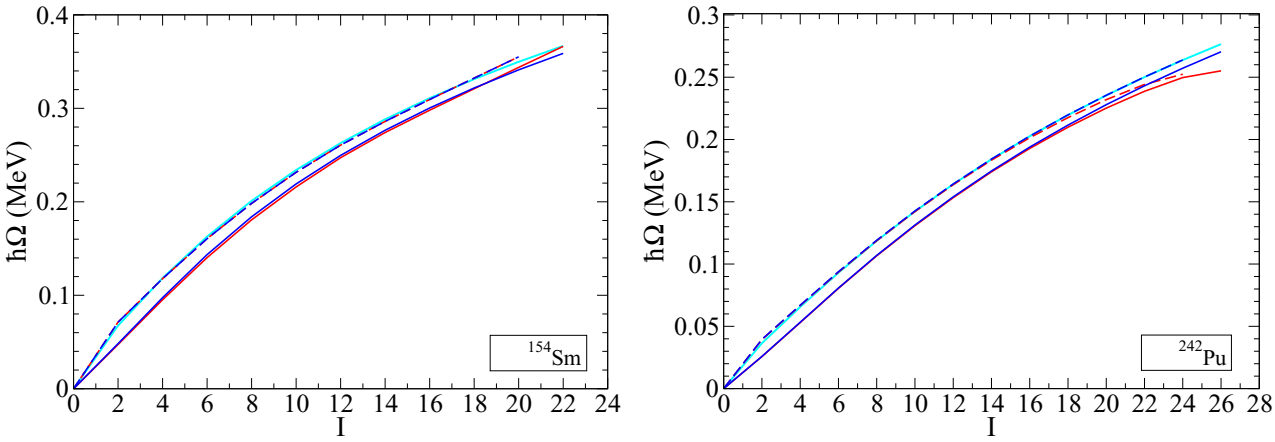

FIG. 7. Comparison between the values of the angular velocity Ω as function of the angular-momentum quantum number I. Ω values extracted from the experimental energy spectrum are in red, with a solid line when using Eq. (A4) and a dashed line when Eq. (A6) has been used. Results of our model calculation are shown in blue and the same convention as far as solid and dashed lines are concerned. The result of the inversion procedure of Eq. (34) is shown with a light-blue solid line.

Starting from an initial guess

$$\begin{pmatrix} k_o \\ \Omega_o \end{pmatrix},$$

the next two-dimensional (2-D) point in the iterative procedure is given by

$$\begin{pmatrix} k_1 \\ \Omega_1 \end{pmatrix} = \begin{pmatrix} k_o \\ \Omega_o \end{pmatrix} - \alpha \vec{\nabla} S|_{k_o,\Omega_o} = \begin{pmatrix} k_o \\ \Omega_o \end{pmatrix} - \alpha \begin{pmatrix} \frac{\partial S}{\partial k}|_{k_o,\Omega_o} \\ \frac{\partial S}{\partial \Omega}|_{k_o,\Omega_o} \end{pmatrix}, \quad \text{(B9)}$$

where the parameter α has to be chosen so as to minimize the function $S(k, \Omega)$ at the given values (k_1, Ω_1).

This procedure does, indeed, converge well, as determined by testing on several nuclei of the rare-earth and the actinide regions, yielding rotational energies that differ from those generated by the method presented in Sec. III B only very marginally, as discussed there.

APPENDIX C: DETERMINATION OF THE ANGULAR VELOCITY AS A FUNCTION OF SPIN

In our model we are able to define an "exact" angular velocity Ω (i.e., without recourse to a derivative approximated by discretization) as the solution of the implicit equation (34). In Fig. 7 we compare the values $\Omega^{(\mathrm{inv})}_{\mathrm{theor}}$ obtained by the inversion of Eq. (34) with those, noted $\Omega^{(sp)}_{\mathrm{theor}}$, deduced either from the experimental or theoretical energy spectra through a derivative approximation, be it by Eq. (A4) or by Eq. (A6). Let us note that, in the latter case this energy spectrum is resulting, through Eq. (5), from the Ω values determined by Eq. (34). This comparison is made for the ^{154}Sm and ^{242}Pu nuclei, taken as relevant examples, since they are not affected by band crossings up to large angular-momentum values. The two theoretical angular velocities, $\Omega^{(sp)}_{\mathrm{theor}}$ on one hand and $\Omega^{(\mathrm{inv})}_{\mathrm{theor}}$ on the other, stem from the same energy model and thus merely differ by the discretization in the variable (I or Ω) for the former while these variables are considered to be continuous for the latter. It turns out that, for both nuclei investigated here, the agreement between theoretical and experimental angular velocities is very good, irrespective of the choice made to extract the Ω values from the spectra [namely, upon using Eq. (A4) or Eq. (A6)]. It is significant that the Ω values (in units of $\hbar$) obtained by the inversion of Eq. (34) coincide almost perfectly with those deduced from their consideration as Lagrange multipliers when calculating $\hbar\Omega$ through the derivative $dE/d\tilde{I}$ according to Eq. (A6). Since they should be formally identical, this agreement simply represents an assessment of the quality of the discretization made when evaluating the double-sided approximate derivative through Eq. (A6).

[1] N. Bjerrum, in *Nernst Festschrift* (Knapp, Halle, 1912), p. 90, quoted in Å. Bohr and B. R. Mottelson, *Nuclear Structure* (World Scientific, Singapore, 1975), Vol II, p. 2.

[2] G. Scharff-Goldhaber, C. B. Dover, and A. L. Goodman, Annu. Rev. Nucl. Sci. **26**, 239 (1976).

[3] R. F. Casten, *Nuclear Structure from a Simple Perspective* (Oxford University Press, Oxford, 1990), Chap. 6, p. 185.

[4] S. M. Harris, Phys. Rev. **138**, B509 (1965).

[5] Å. Bohr, B. R. Mottelson, and D. Pines, Phys. Rev. **110**, 936 (1958).

[6] A. B. Migdal, Nucl. Phys. **13**, 655 (1959).

[7] S. T. Belyaev, Nucl. Phys. **24**, 322 (1961).

[8] S. G. Nilsson, O. Prior, and K. Dan. Vidensk. Selsk. Mat. Fys. Medd. **32**, 1 (1961).

[9] J. J. Griffin and M. Rich, Phys. Rev. **118**, 850 (1960).

[10] O. Prior, F. Boehm, and S. G. Nilsson, Nucl. Phys. A **110**, 257 (1968).

[11] B. R. Mottelson and P. G. Valatin, Phys. Rev. Lett. **5**, 511 (1960).
[12] B. Nerlo-Pomorska, K. Pomorski, and J. Bartel, Phys. Rev. C **84**, 044310 (2011).
[13] B. Nerlo-Pomorska, K. Pomorski, and J. Bartel, Int. J. Mod. Phys. E **21**, 1250050 (2011).
[14] B. Nerlo-Pomorska, K. Pomorski, P. Quentin, and J. Bartel, Phys. Scr. **84**, 044310 (2014).
[15] P. Quentin, H. Lafchiev, D. Samsoen, and I. N. Mikhailov, Phys. Rev. C **69**, 054315 (2004).
[16] S. Chandrasekhar, *Elipsoidal Figures of Equlibrium* (Dover, New York, 1987).
[17] P. Quentin and J. Bartel, Bulg. J. Phys. **44**, 326 (2017); P. Quentin, J. Bartel, L. Bonneau, M.-H. Koh, N. M. Nor, N. A. Rezle, and K.-W. K. Lee, *ibid.* **46**, 326 (2019).
[18] I. N. Mikhailov, P. Quentin, and D. Samsoen, Nucl. Phys. A **627**, 259 (1997).
[19] D. Vautherin, Phys. Rev. C **7**, 296 (1973).
[20] M. Tinkham, *Introduction to Superconductivity*, Second Edition (Mc Graw-Hill, New York, 1996), p. 63.
[21] K. Bencheikh, P. Quentin, and J. Bartel, Nucl. Phys. A **571**, 518 (1994).
[22] J. Bartel, P. Quentin, M. Brack, C. Guet, and H.-B. Håkansson, Nucl. Phys. A **386**, 79 (1982).
[23] M. Beiner, H. Flocard, N. Van Giai, and P. Quentin, Nucl. Phys. A **238**, 29 (1975).
[24] R. W. Hasse and W. D. Myers, *Geometrical Relationships of Macroscopic Nuclear Physics* (Springer, 1988).
[25] W. D. Myers and W. J. Swiatecki, Nucl. Phys. **81**, 1 (1966).
[26] S. Raman, C. W. Nestor, and P. Tikkanen, At. Data Nucl. Data Tables **78**, 1 (2001).
[27] J.-P. Delaroche, M. Girod, J. Libert, H. Goutte, S. Hilaire, S. Peru, N. Pillet, and G. F. Bertsch, Phys. Rev. C **81**, 014303 (2010); see Table at http://www-phynu.cea.fr/HFB-5DCH-table.htm
[28] J. Bardeen, N. Cooper, and J. R. Schrieffer, Phys. Rev. **108**, 1175 (1957).
[29] C. Kittel, *Quantum Theory of Solids* (John Wiley & Sons, New York, 1963).
[30] S. G. Nilsson, C. F. Tsang, A. Sobiczewski, Z. Szymański, S. Wyceh, S. Gustafson, I.-L. Lamm, P. Möller, and B. Nilsson, Nucl. Phys. A **131**, 1 (1969).
[31] N. Pillet, P. Quentin, and J. Libert, Nucl. Phys. A **697**, 141 (2002).
[32] N. Pillet, J.-F. Berger, and E. Caurier, Phys. Rev. C **78**, 024305 (2008).
[33] National Nuclear Data Center, *Chart of Nuclides* (Brookhaven National Laboratory, Upton); https://www.nndc.bnl.gov/nudat2/
[34] J. Dobaczewski, P. Magierski, W. Nazarewicz, W. Satuła and Z. Szymański, Phys. Rev. C **63**, 024308 (2001).
[35] T. Duguet and T. Lesinski, AIP Conf. Proc. **1165**, 243 (2009).
[36] H. Laftchiev, D. Samsoen, P. Quentin, and I. N. Mikhailov, Phys. Rev. C **67**, 014307 (2003).
[37] M. J. A. de Voigt, J. Dudek and Z. Szymański, Rev. Mod. Phys. **55**, 949 (1983).
[38] U. Mosel, J. Phys., Colloq. **41**, C10-253 (1980).
[39] M. Bender, P.-H. Heenen, and P.-G. Reinhard, Rev. Mod. Phys. **75**, 121 (2003).